Tellus (2007), 59A, 261–272
Printed in Singapore. All rights reserved

TELLUS

Northern Hemisphere sea ice variability: lag structure and its implications

By JINRO UKITA[1]*, MEIJI HONDA[2,3], HISASHI NAKAMURA[2,4], YOSHIHIRO TACHIBANA[2,5], DONALD J. CAVALIERI[6], CLAIRE L. PARKINSON[6], HIROSHI KOIDE[7] and KENTARO YAMAMOTO[7], [1]*Lamont-Doherty Earth Observatory of Columbia University, Palisades, NY 10964, USA;* [2]*Frontier Research Center for Global Change, Japan Agency for Marine-Earth Science and Technology Center, Yokohama, 236, Japan;* [3]*International Research Institute for Climate Prediction, Palisades, NY 10964, USA;* [4]*Department of Earth and Planetary Science, University of Tokyo, Tokyo, 113, Japan;* [5]*Liberal Arts Education Center, Tokai University, Hiratsuka, 259, Japan;* [6]*NASA Goddard Space Flight Center, Greenbelt, MD 20771, USA;* [7]*Japan Meteorological Agency, Tokyo, 100, Japan*

(Manuscript received 4 August 2005; in final form 30 November 2006)

ABSTRACT

An analysis of satellite sea-ice records for recent decades reveals a highly coherent spatial and temporal structure of the Northern Hemisphere (NH) wintertime sea-ice variability and its close link to anomalous atmospheric circulation. The dominant mode of the wintertime sea-ice variability is characterized by a double-dipole composed of one dipole over the North Atlantic and the other over the North Pacific, which are mutually correlated interannually. This dominant sea-ice mode is lag correlated with the winter-averaged North Atlantic Oscillation (NAO) index at lags up to two winters when the NAO leads. In the sub-Arctic, significant lead–lag relationships exist between sea-ice extent (SIE) anomalies on regional scales, which are closely associated with atmospheric circulation anomalies. An eastward evolving pattern is identified in regional SIE anomalies from the Labrador to Nordic and farther to the Okhotsk Sea at multi-year time-scales, led by anomalously weak Aleutian and strong Icelandic lows. The results suggest the presence of climate memories over the North Atlantic and Eurasia, which are crucial for recent downward trends in the NH SIE by transforming atmospheric influences into slower changes in sea-ice conditions. The summer Okhotsk high, which leads to a sea-ice reduction along the east Siberian coast and further affects sea-ice conditions over the Arctic Ocean, is a key link between summer Arctic and winter sub-Arctic sea-ice trends. We also conjecture that variations and changes in the NH sea-ice conditions are linked to climate variability in the tropics.

1. Introduction

Sea ice covers most of the Arctic Ocean and its adjacent seas in the boreal winter. Since the region is a major pathway of global freshwater transport, Northern Hemisphere (NH) sea-ice is of significant importance to the global water cycle (Aagaard and Carmack, 1989; Wijffels et al., 1992). Sea ice also plays a fundamental role in the global energy balance (Overland and Turet, 1994), as it is highly reflective of solar radiation and limits the transfer of energy, moisture, and momentum between the ocean and the atmosphere. From these and other climatic considerations, the NH sea-ice cover is recognized as an important component of the global climate system. Over the past three decades, the areal extent of NH sea-ice has decreased at a rate of about 3% per decade on an annual basis, which exhibits strong seasonal dependence with much larger trends in summer than in winter (Parkinson et al., 1999; Cavalieri et al., 2003). Previous studies have also indicated strong regional dependence in sea-ice cover trends and hinted at the presence of a spatially coherent sea-ice anomaly pattern among geographically separated regions for the winter season (Parkinson et al., 1999). In light of a possible link between global warming and climate changes, especially those observed in northern high latitudes in recent decades (e.g. Walsh et al. 1996; Watanabe and Nitta 1998; Dickson et al., 2000; Serreze et al., 2000; Rothrock et al., 2003; Stroeve et al., 2005, among others), sea-ice trends and variability are of major concern in climate research.

Northern Hemisphere wintertime sea-ice variability has a component that appears to be closely associated with the North Atlantic Oscillation (NAO). The NAO refers to a recursive

*Corresponding author.
e-mail: jukita@faculty.chiba-u.jp
Present address: Center for Environmental Remote Sensing, Chiba University, 1-33 Yayoi, Chiba, Japan 263-8522.
DOI: 10.1111/j.1600-0870.2006.00223.x

pattern of anomalies in surface westerlies over the North Atlantic and is closely associated with a seesaw between the intensities of the climatological Icelandic low and the Azores high (e.g. van Loon and Rogers, 1978; Rogers and van Loon, 1979; Chapman and Walsh, 1993; Hurrell, 1995; Parkinson, 2000). Recent studies have revealed a connection between the NAO and the first empirical orthogonal function (EOF) mode of the NH wintertime sea-ice variability (Deser et al., 2000; Partington et al., 2003, and references therein). However, questions remain as to the exact relationship of NH sea-ice variability to prominent regional and hemispheric modes of atmospheric variability, in particular to the NAO and the Arctic Oscillation (AO). The AO, or the NH annular mode, is defined as the leading EOF of the wintertime monthly sea level pressure (SLP) anomaly field north of 20°N (Thompson and Wallace, 1998). Wallace (2000) considered the AO as a hemispheric atmospheric mode in which the NAO is embedded as a regional manifestation.

Despite the presence of strong temporal covariability between the leading EOF of NH sea-ice variability and the NAO, their corresponding spatial patterns differ appreciably. For example, the spatial patterns of the leading EOF of the wintertime sea-ice concentration (SIC) field and its projection on the wintertime SLP anomaly field are not confined to the Euro-Atlantic sector, which is regarded as the domain for the NAO. A secondary centre of action appears over eastern Siberia in the anomalous SLP field associated with the leading EOF of the winter SIC (e.g. fig. 2 of Deser et al., 2000). Notably, the location of this signature differs from that of the Pacific signature of the AO, which lies over the eastern North Pacific. Based on an EOF analysis of the year-round weekly-mean NH SIC field, Partington et al. (2003) identified that the leading EOF of the SIC field is a winter mode, which is significantly lag correlated with the NAO index (leading by one winter), but not so significantly correlated with the AO index. These previous findings suggest what appear to be subtle, yet complex, relationships in both space and time among the leading wintertime sea-ice mode, the NAO and the AO.

In this study, we extend the previous results and investigate details of the temporal and spatial characteristics of the NH winter-to-winter sea-ice variability using fully hemispheric satellite records over the period 1979–2003. In particular, we examine the extent to which NH wintertime sea-ice variability has coherent hemispheric-scale structure and whether there are significant lag relationships both between sea-ice anomalies in different regions and between these sea-ice and atmospheric circulation anomalies. We further attempt to identify a sequence of anomalies in sea-ice and atmospheric circulation with the focus on spatial scales roughly equal to regions the size of the Labrador Sea and on temporal scales longer than a season.

2. Data and methodology

Sea-ice data used in this study, which cover the period 1979–2003, are derived from the Scanning Multichannel Microwave Radiometer (SMMR) onboard the Nimbus 7 satellite and the Special Sensor Microwave Imager (SSMI) onboard satellites of the Defense Meteorological Satellite Program (Cavalieri et al., 1999; Parkinson et al., 1999). For atmospheric data, we use Trenberth's NH monthly SLP data (obtained from dss.ucar.edu/datasets/ds010.1 and earlier data described in Trenberth and Paolino, 1980). The NAO index is defined as the normalized difference in normalized December–March mean SLP between Lisbon and Stykkisholmur (Hurrell, 1995) and is obtained from the Joint Institute for the Study of the Atmosphere and Ocean of the University of Washington (jisao.washington.edu/data).

'Sea-ice concentration' is defined as the percentage of sea-ice cover in the area of interest, here divided into grid cells of 25 km by 25 km in size, whereas 'sea-ice extent' (SIE) is the cumulative area of all grid cells with at least 15% ice concentration for a prescribed domain. Unless otherwise stated, the 'Sea of Okhotsk' refers to the combined domain of the Seas of Okhotsk and Japan, the 'Labrador Sea' refers to the Baffin Bay and the Labrador Sea, and the 'Nordic Seas' refers to the Greenland, Barents, and Kara Seas [see plate 1 of Parkinson et al. (1999) for exact geographical locations of these areas]. All sea-ice data are averaged over the February–March period, which corresponds to the time of the maximum sea-ice cover in the NH. Based on this winter data set, this study focuses on wintertime sea-ice variability at interannual time-scales with extended discussions on NH sea-ice trends and summertime variability. Since there are trends in many of the time-series used in this study, we have removed linear trends prior to computing regressions and correlations; for example, trends are removed from the SLP anomaly field at individual grid squares. In the analyses, which cover the 25 winters in the period 1979–2003, correlation coefficients whose absolute values exceed 0.40 and 0.50 are considered significant at the 95% and 99% confidence levels, respectively, based on the two-sided *t*-test.

3. Results

3.1. Spatial structure

Figure 1a shows the dominant sea-ice anomaly pattern extracted through an EOF analysis applied to the covariance matrix of NH SIC anomalies averaged over the February–March period, which accounts for 27% of the total variance of the SIC field. This pattern represents a seesaw in anomalous sea-ice cover between the eastern and western hemispheres, with one polarity (phase) in the Sea of Okhotsk and the Nordic Seas and the opposite polarity in the Bering and Labrador Seas (Table 1).

In order to examine the extent to which this SIC anomaly pattern reflects variations in regional SIEs, we applied the same EOF analysis to a four-variable system composed of the regional SIE time-series of the Labrador, Nordic, Bering and Okhotsk Seas, which are identified as action centres in Fig. 1a. The principal

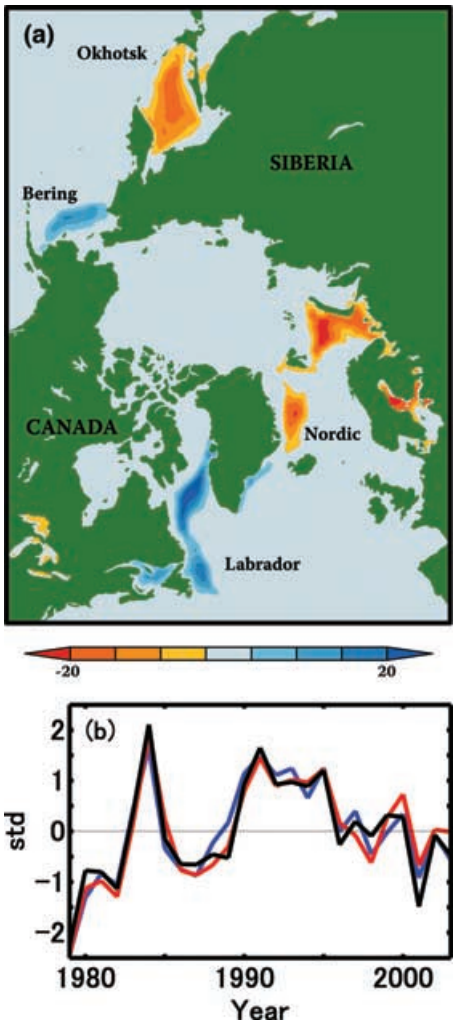

Fig. 1. Leading mode of sea-ice variability. (a) First EOF of the winter (February–March) mean NH SIC field. The colour indicates the local change in SIC in per cent for one unit standard deviation increase in the PC1 time-series. (b) Normalized principal component time-series for the first EOF modes of the SIC field (blue) and the four-region SIE field (PC1-SIE; red), and the normalized algebraic mean of the North-Atlantic and North-Pacific SIE seesaw indices (black). The time-series prior to de-trending are shown.

component time-series corresponding to the first EOF of the SIE variability (hereafter referred to as PC1-SIE to distinguish it from other leading EOFs of sea-ice variability) is virtually identical to its counterpart for the SIC variability ($r = 0.95$, Fig. 1b). PC1-SIE accounts for 59% of the total variance of this four-variable system of the regional SIEs and is significantly correlated with each of the four regional SIE time-series (Table 1). When those four regional SIE time-series are added to form a single sub-Arctic SIE time-series, its correlation with the NH total SIE time-series is highly significant ($r = 0.97$ for de-trended time-series). The above results indicate that the sub-Arctic is the region in which winter sea-ice variability is highly concentrated, whose spatial and temporal variations are well represented by PC1-SIE.

Most previous studies have focused primarily on regional aspects of the double-seesaw pattern associated with PC1-SIE either for the North Atlantic or for the North Pacific (e.g. Rogers and van Loon, 1979; Parkinson, 1990; Chapman and Walsh, 1993; Niebauer, 1998). For example, these studies have examined a sea-ice seesaw between the Labrador Sea and the Nordic Seas in the Atlantic sector and/or another sea-ice seesaw between the Bering Sea and the Sea of Okhotsk in the Pacific sector. In order to investigate how coherently North Atlantic and North Pacific sea-ice variations contribute to the aforementioned hemispheric double-seesaw pattern, we constructed a pair of difference time-series of the regional SIEs, one for the North Atlantic and the other for the North Pacific. Here the North-Atlantic SIE seesaw index is defined as the normalized difference in the normalized February–March mean SIE time-series between the Labrador and Nordic Seas (Labrador minus Nordic). Similarly, the North-Pacific SIE seesaw index is defined as the normalized difference in the normalized Bering and Okhotsk SIE time-series (Bering minus Okhotsk). These North-Atlantic and North-Pacific SIE seesaw indices are correlated at the 99% confidence level ($r = 0.55$ with trends and 0.54 after removing their trends). Their algebraic mean is highly correlated with PC1-SIE (Fig. 1b, $r = 0.96$). The correlations of PC1-SIE with the North-Atlantic and North Pacific SIE seesaw indices are significant ($r = 0.93$ and 0.74, respectively, with trends and 0.95 and 0.75 after removing trends). The hemispheric SIE double-seesaw pattern thus consists of the mutually linked North-Atlantic and North-Pacific regional seesaws with a greater contribution from the former.

Table 1. Statistics of February–March averaged regional SIEs and their correlations with the leading mode of sea-ice variability

Region	Mean area (10^6 km^2)	Standard deviation (10^6 km^2)	Correlation with PC1-SIE w/ trends	Correlation with PC1-SIE de-trended
Labrador	1.40	0.16	0.67	0.82
Nordic	2.68	0.22	−0.89	−0.90
Okhotsk	1.15	0.17	−0.71	−0.70
Bering	0.72	0.10	0.47	0.50
Combined	5.97	0.27	−0.59	−0.51

The variation in the spatial extent of the NH sea-ice in winter is closely related to that in large-scale atmospheric circulation through anomalous winds, which lead to anomalous surface air temperature advection and ice drift (see discussion in Deser et al., 2000 and references therein). Deser et al. (2000) noted that there is a delay in the sea-ice response to atmospheric forcing by weeks. We also find a similar delayed relationship between PC1-SIE (based on February–March data) and the NAO index. When Hurrell's winter mean (based on December-to-March) NAO index is used, their correlation is 0.52. In comparison, the correlation of PC1-SIE with the monthly NAO index shows its maximum in January ($r = 0.50$), while the corresponding correlation is 0.32, 0.31 and -0.07 for December, February and March, respectively. On the basis of these findings, we subsequently use the December–January–February (DJF) mean SLP anomaly field to investigate a linkage between the variations in the atmosphere and in mid-winter sea-ice.

The maps of DJF mean SLP anomalies regressed linearly on the PC1-SIE, North-Atlantic, and North-Pacific SIE seesaw indices (Figs. 2a–c) consistently show anomaly centres over eastern Siberia in addition to NAO-like dipoles in the Euro-Atlantic sector. Although Deser et al. (2000) noted this Siberian feature (their fig. 2), the sea-ice data used in their analysis did not cover a large section of the Sea of Okhotsk, whose contributions to the NH sea-ice variability and to the leading sea-ice mode are far from negligible (see Table 1). Thus, this study, based on fully hemispheric sea-ice records, for the first time confirms the presence of the hemispheric-scale sea-ice double seesaw pattern and associated SLP anomalies in the North Atlantic and eastern Siberia.

3.2. Lag structure

Table 2 shows lagged cross-correlations of Hurrell's NAO index (leading) with various sea-ice indices discussed above. As reported in Partington et al. (2003), the lagged cross-correlation between PC1-SIE and the NAO index of the previous winter is significant ($r = 0.56$). Intriguingly, the correlation is significant ($r = 0.54$) even for a lag of two winters, whereas no significant correlation is found with the time-lag longer than two winters or for the case when PC1-SIE leads the NAO index. Consistent with those significant lagged correlations, the linear regression maps of DJF mean SLP anomalies on PC1-SIE with one and two winters of lag (Figs. 2d and 2g, respectively) show North Atlantic dipoles resembling the positive phase of the NAO. In addition, there are positive SLP anomalies in the North Pacific, which are more significant with the biennial lag. In comparison with the Siberian signature of Figs. 2a–2c, the Pacific anomalies in Figs. 2d and 2g are located near the Aleutian Islands as is the case for the AO.

Since PC1-SIE is correlated with the North-Atlantic and North-Pacific SIE seesaw indices ($r = 0.95$ and 0.75, respectively) and with each of the regional SIE time-series (Table 1), the aforementioned lag relationships can be examined through further correlation and regression analyses of SLP anomalies with the basin- and regional-scale SIE time-series. For example, Fig. 2e shows the map of DJF mean SLP anomalies (leading) regressed on the North-Atlantic SIE seesaw index with a lag of one winter. The spatial pattern of the SLP anomalies resembles its counterpart in Fig. 2d, particularly in the Euro-Atlantic region. This result suggests that the lag relationship between the NAO and PC1-SIE is a manifestation of the delayed influence of the NAO-like pressure dipole on the North-Atlantic sea-ice seesaw. The lagged correlation between the NAO (leading) and North-Atlantic sea-ice seesaw indices with a lag of one winter ($r = 0.61$ and significant at the 99% confidence level) further supports this view.

Even with a biennial lag being imposed, the regression map of DJF mean SLP anomalies (leading) on the North-Atlantic seesaw index (Fig. 2h) exhibits an anomaly pattern similar to that in Fig. 2g. In comparison, the North-Pacific counterpart (Fig. 2i) displays no significant SLP dipole pattern in the North Atlantic. Rather, it exhibits a clear dipole pattern between the Arctic and the North Pacific with a particularly strong North Pacific signature. The spatial pattern of Fig. 2g, especially its Pacific signature, is traced to this North Pacific signal in Fig. 2i. Given the definition of the North-Pacific SIE seesaw index (Bering minus Okhotsk), the North-Pacific signature of Figs. 2g and 2i can then be traced to a lag relationship of SLP anomalies in the North Pacific (leading by two winters) with the Okhotsk SIE, as shown in Fig. 3c. Note that the minus sign in the SLP anomalies is consistent with the minus sign in the definition of the North-Pacific SIE seesaw index with respect to the Okhotsk SIE.

A further analysis of the lead–lag relationships between regional SIE anomalies reveals an eastward evolving pattern of regional SIE anomalies and associated large-scale circulation anomalies. Two winters prior to the time (at $t = -2$ yr) of anomalously positive PC1-SIE, the NAO tends to be in its positive phase, characterized by an intensified Icelandic low, along with a weakened Aleutian low (Fig. 2g). Associated with the positive phase of the NAO, the Labrador and Nordic SIEs tend to be above- and below-normal, respectively (see Table 2 and Fig. 3a). However, this anomalous pattern of the regional SIEs in the North Atlantic is peaked in the following winter (at $t = -1$ yr) especially for the Nordic Sea. For example, the lagged correlation between the NAO (leading) and the Nordic SIE time-series with a lag of one winter is more significant than that without a lag ($r = -0.56$ compared with $r = -0.48$). Accompanied by this is a significant lag relationship between the Labrador (leading by one winter) and Nordic SIEs ($r = -0.63$). Figure 4a clearly shows this lag relationship in regional SIE anomalies over the subpolar North Atlantic, and the map of DJF mean SLP anomalies (leading) on the Nordic SIE time-series at a lag of one winter (Fig. 3b) further shows both the North Atlantic atmospheric dipole and the anomalies in the northern North Pacific.

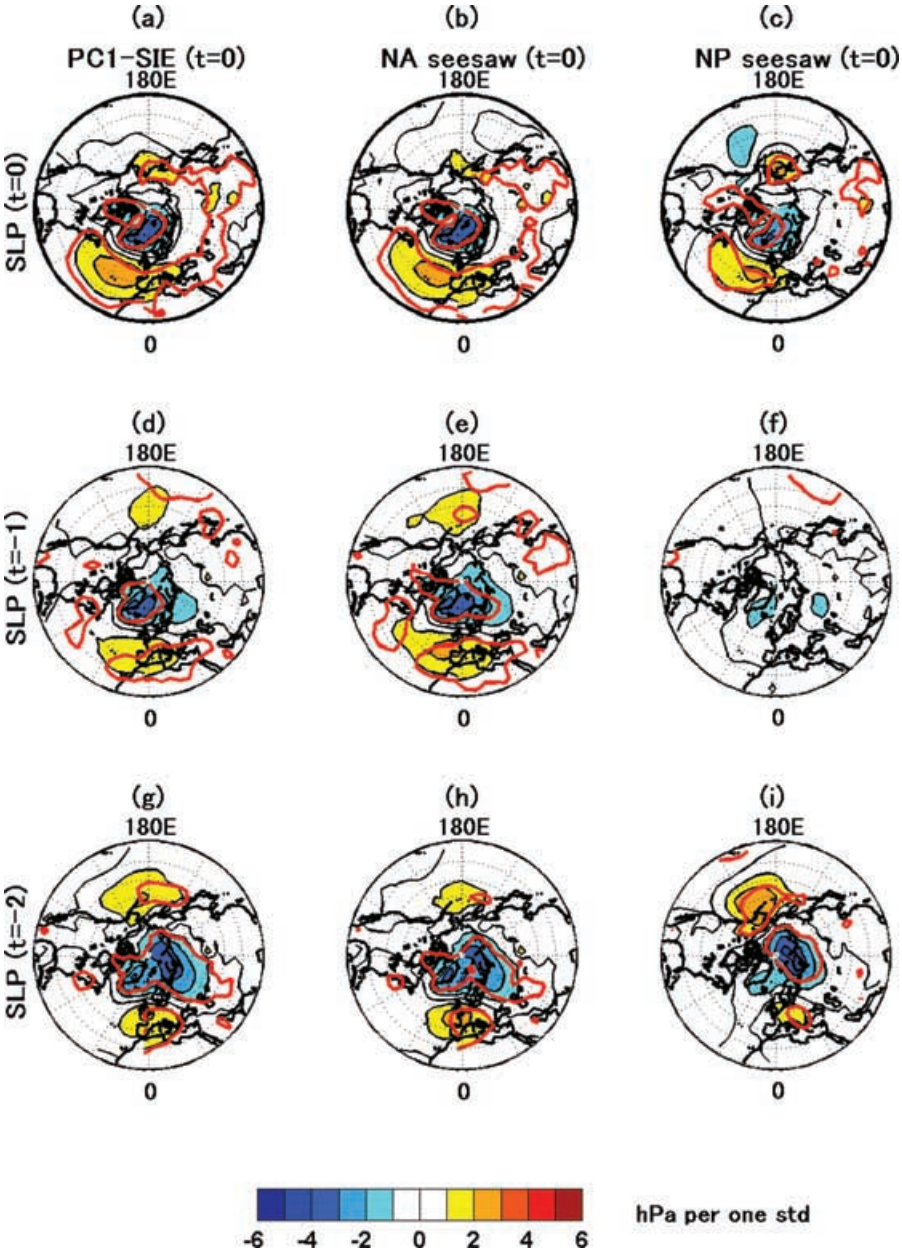

Fig. 2. Maps of the linear regression coefficients of winter (DJF) averaged SLP anomalies on (a) PC1-SIE, (b) North-Atlantic SIE seesaw, and (c) North-Pacific SIE seesaw indices (all are detrended). (d)–(i) the same as (a)–(c) but with lags. SLP anomalies lead sea-ice indices by one winter [second row, (d)–(f)] and by two winters [third row, (g)–(i)]. Three sea-ice indices are PC1-SIE (first column), the North-Atlantic SIE seesaw index (second column), and the North-Pacific SIE seesaw index (third column). The units on the colour scaling are hPa per one standard deviation for each of the normalized time-series. The maps are on polar-stereographic projections and include all latitudes polewards of 20°N. The red contours outline the areas with >95% confidence level.

As an extended part of the evolving pattern of regional SIE anomalies, there appears a lag relationship from the Nordic SIE (leading at $t = -1$ yr) to the Okhotsk SIE (at $t = 0$). For the period of 1979–2003, the lag correlation between these regional SIEs is 0.31. However, the Okhotsk SIE in 2001 is an extreme outlier as indicated by an open square in Fig. 4b, which strongly affects estimates in our linear regression and correlation analyses. Without this outlier the correlation is 0.48 (significant at the 95% level); no other points have such a high degree of leverage to affect the estimates. The relevance of the Okhotsk SIE to the above eastward pattern is also evidenced by the regression map of DJF mean SLP anomalies (leading) on the Okhotsk SIE time-series with a lag of two winters (Fig. 3c). It shows a spatial pattern consisting of negative anomalies in

Table 2. Lagged cross-correlations between the NAO index (leading) and various sea-ice time-series. All calculations are based on de-trended time-series. The numbers in parentheses indicate corresponding figures

Lag	PC1-SIE	North Atlantic seesaw	North Pacific seesaw	Labrador SIE	Nordic SIE	Okhotsk SIE	Bering SIE
No lag	0.52 (2a)	0.56 (2b)	0.42 (2c)	0.52 (3a)	−0.48	−0.22	0.46
One winter	0.56 (2d)	0.61 (2e)	0.15 (2f)	0.55	−0.56 (3b)	−0.30	−0.06
Two winters	0.54 (2g)	0.52 (2h)	0.31 (2i)	0.47	−0.46	−0.44 (3c)	0.06

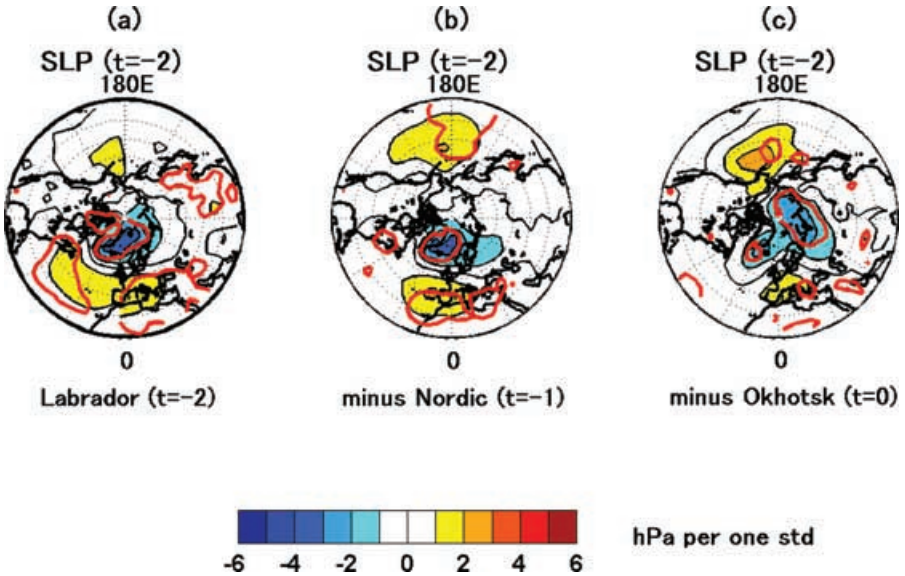

Fig. 3. Maps of the linear regression coefficients of winter (DJF) averaged SLP anomalies (leading) on (a) the Labrador SIE times series without a lag, (b) the Nordic SIE time-series lagged by one winter, and (c) the Okhotsk SIE time-series lagged by two winters. The signs for (b) and (c) are reversed since the Nordic and Okhotsk SIE time-series are negatively correlated with the NAO index and PC1-SIE with a lag (see Table 2), while the Labrador SIE time-series is not.

the subpolar North Atlantic and positive anomalies in the North Pacific.

Although de-trended data were used throughout our regression and correlation analyses to minimize possible contaminations arising from sampling biases, uncertainties remain due to the 25-year length of the sea-ice record. Because of our particular concern about the outlier issue of Fig. 4b, we examined longer sea-ice records of the Okhotsk Sea (not including the Sea of Japan) compiled by the Japan Meteorological Agency for the period 1971–2000. For this longer time-series extending back to 1971, the regression of DJF mean SLP anomalies (leading) on the Okhotsk SIE time-series with a lag of two winters produces a spatial pattern similar to that in Fig. 3c. When this extended Okhotsk sea-ice time-series is compared with the Barents sea-ice records for the same period (Vinje, 2001), it turns out that the Barents SIE (leading by one winter) is significantly lag correlated with the Okhotsk SIE ($r = 0.55$ and see Fig. 4c). In addition, this Barents SIE time-series is significantly correlated with the NAO index when the NAO leads by one winter ($r = -0.46$). These analyses add further credibility to our results, in particular the suggestion of an eastward moving pattern of sea-ice anomalies from the Labrador Sea to the Nordic Seas and farther onto the Sea of Okhotsk at multi-year time-scales.

4. Discussion

4.1. Propagating signals

An important question concerning Arctic climate changes in recent decades (e.g. Walsh et al., 1996; Watanabe and Nitta, 1998; Dickson et al., 2000; Serreze et al., 2000; Rothrock et al., 2003; Stroeve et al., 2005, among others) is whether the changes are part of internal decadal-scale oscillations within the Arctic atmosphere-ice-ocean system (e.g. Ikeda, 1990; Mysak and Venegas, 1998) or are a high-latitude response to hemispheric-scale climate change (Watanabe and Nitta, 1998, 1999; Bengtsson et al., 2004, for relevant discussions). Placing it in a larger perspective, we are interested in knowing whether a sequence of anomalous events, or climatic signals, can be detected in northern mid-to-high latitudes. The presence of such signals,

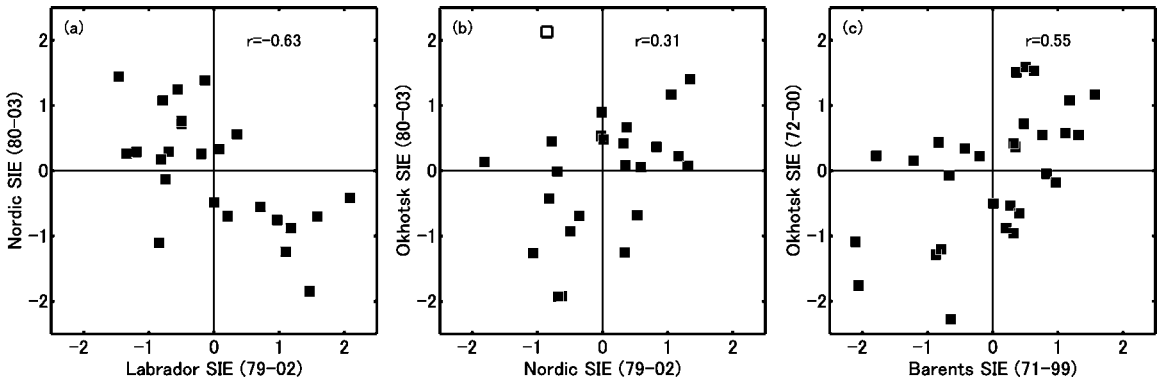

Fig. 4. Scatter plots for the lag relationships between regional SIEs. (a) The Labrador SIE versus the Nordic SIE when the Labrador SIE leads by one winter. (b) The Nordic SIE versus the Okhotsk SIE when the Nordic SIE leads by one winter. (c) The Barents SIE versus the Okhotsk SIE when the Barents SIE leads by one winter. (a) and (b) are based on the NASA sea-ice records for 1979–2003, and (c) is for 1971–2000 and based on the wintertime Barents sea-ice records of Vinje (2001) and the Japan Meteorological Agency's (JMA) wintertime Okhotsk sea-ice records, which do not include SIE in the Sea of Japan. All plots are based on normalized and de-trended SIE time-series

especially those at multi-year to subdecadal time-scales, would provide important clues on underlying causes and mechanisms of the recent Arctic climate changes.

Observations and modelling results have frequently indicated the propagating and persistent characteristics of various climatic signals over the North Atlantic on multi-year time-scales. For example, many of the hydrographic time-series in the Nordic seas exhibit strong lag correlations with the NAO time-series with multi-year lags (e.g. Blindheim et al, 2000). Other investigators have shown sea-ice anomalies evolving within the subpolar North Atlantic on time-scales of a season to multiple years (e.g. Deser et al., 2002). They also discussed a possible linkage between sea-ice anomalies and multi-year persistence in SST anomalies, which may result from the re-emergence mechanism of SST anomalies (e.g. Deser et al., 2003, and references therein). This mechanism refers to an air–sea coupled process by which SST anomalies generated in winter survive to re-emerge in the following winter. A memory is provided by anomalous heat content entering in the winter mixed-layer and subsequently stored beneath the shallower summertime mixed-layer, which in turn could affect sea-ice formation in a subsequent winter.

On the basis of observations and model results, Kauker et al. (2003) argued that the leading mode of the wintertime sea-ice variations within the combined domain of the subpolar North Atlantic and Arctic Ocean is a delayed response to the AO and further attribute its propagating and persistent characteristics to oceanic heat transport and the re-emergence mechanism of SST anomalies. Combined with those previous results, we interpret our results as suggesting that a part of the biennial lagged relationship between the atmospheric anomalies in the form of the North Atlantic dipole and the leading mode of sea-ice variability is accounted for by regional-scale climatic memory within the subpolar North Atlantic atmosphere–ice–ocean coupled system. In this context, it is of fundamental importance that the autocorrelation of the North-Atlantic sea-ice dipole is significant with a lag of one winter ($r = 0.63$ for both the non-detrended and de-trended time-series). Yet, the autocorrelation of the NAO index is not significant on this time-scale ($r = 0.17$ for a lag of one winter). The difference between those atmospheric and sea-ice autocorrelations in addition to the lag relationship between the NAO and North-Atlantic sea-ice seesaw indices (Table 2) seems to indicate a forcing role of the atmosphere and the presence of climatic memory in the atmosphere–ice–ocean coupled system over the region.

If contemporaneous and lagged sea-ice relationships between the North Atlantic and the Sea of Okhotsk, which lies east of the Eurasian continent, are real and not artifacts from statistical analyses, there arises the question of whether there is also a regional climatic memory over Eurasia. Given the short intrinsic time-scale of the troposphere, if such memory were to exist, it is likely related to variations and changes in surface conditions. Some authors have discussed a lag relationship between the NAO and anomalous snow-cover over Eurasia (e.g. Cohen and Entekhabi, 1999; Bojariu and Gimeno, 2003; Robock et al., 2003). Model results support the presence of a physical link between anomalous snow-cover and atmospheric circulation (Watanabe and Nitta, 1999). Ogi et al. (2004a) argued that the Nordic Seas, particularly the Barents Sea, may be a forcing region of anomalous summertime atmospheric circulation affecting the downstream regions. The results from those previous and present studies appear to support the notion of climatic memory across the Euro-Atlantic sector and Eurasia, although much work is needed to understand specific mechanisms for the observed signals and the relative importance of the different mechanisms.

Our results on the spatial and lag structure of sea-ice variability and associated anomalous atmospheric circulation shed new light on the widely reported recent downward trends in the NH sea-ice cover for both winter and summer. For winter the trend is predominantly a result of the decreasing trend in the Nordic Seas

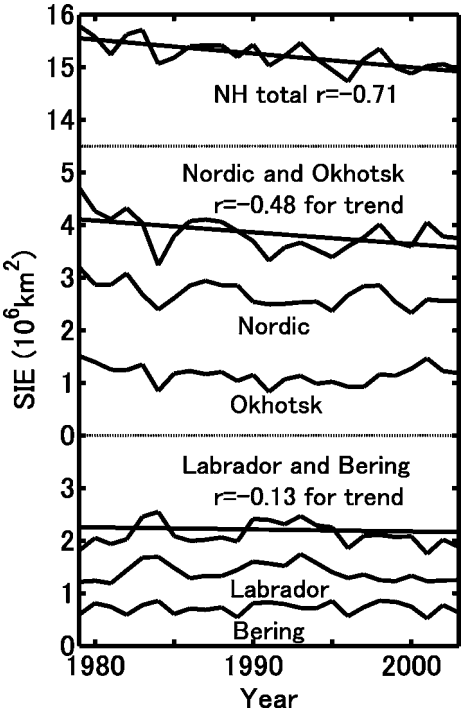

Fig. 5. Comparison of regional winter (February–March) mean SIE time-series for the period 1979–2000. The top panel shows the NH total SIE time-series. The middle panel shows the Nordic, Okhotsk, and their combined (summed) SIE time-series. The bottom panel shows the Labrador, Bering, and their combined SIE time-series. The solid lines indicate the linear trends in the NH total and combined time-series. The linear trend of the combined Nordic and Okhotsk SIEs is significant at the 99% confidence level ($r = 0.60$) based on the two-sided t-test.

(Fig. 5), which is not counterbalanced by the trends in other sub-Arctic regions (e.g. the comparison between the top, middle and bottom parts of Fig. 5). An important factor in this explanation is that the Nordic Seas region as a whole is the largest in area among the four main sub-Arctic regions (see Table 1). Thus, it tends to dominate other regions in trend statistics. It is also significant that the Nordic and Okhotsk SIEs, which together account for about two-thirds of the sub-Arctic regions, tend to vary in alignment with each other at subdecadal to decadal timescales (e.g. Parkinson et al., 1999; Parkinson, 2000).

Our results suggest that several factors jointly contribute to the NH wintertime sea-ice trend. The magnitude and frequency of high-NAO events are important since the positive-NAO tends to result in a reduced sea-ice cover in the Nordic Seas, which dominate the sub-Arctic region in area as mentioned above. In addition, two factors, the persistence of the North-Atlantic sea-ice dipole with respect to the NAO and the positive lag relationship between the North-Atlantic sea-ice dipole and the lagged Okhotsk sea-ice variation, act to prolong and disseminate atmospheric influences over a large part of the sub-Arctic region.

4.2. Winter-to-summer link

While the downward trend in the wintertime NH SIE is a consequence of a sea-ice reduction in the sub-Arctic, the downward trend in the summertime NH SIE results from a reduction in the Arctic Ocean, which has exhibited sharp decreases in recent years (Comiso, 2002; Stroeve et al., 2005 and references therein). Serreze et al. (2001) noted that the enhancement of the Arctic frontal zone along the east Siberian coasts, an area of high storm activity in summer, could bring about this summer sea-ice reduction via combined effects of warm air advected from inland and the break-up of the sea-ice field. Rigor and Wallace (2004) pointed out that the summer sea-ice trend is not spatially homogeneous. In particular, the earlier (1979–1996) trends were concentrated in the Eurasian side of the Arctic Ocean, while the post–2002 record minima in the summer SIE of the Arctic Ocean were concentrated in the Alaskan coastal region in addition to the Eurasian side (see their fig. 1). Rigor and Wallace further argued that an episodic high-AO event of 1989–1990 and subsequent atmospheric conditions in the early 1990s considerably altered the sea-ice thickness distribution towards a younger and thinner sea-ice cover, which led to a retreat of the ice-edge in recent summers after being advected into the Alaskan coastal region.

Model studies suggest that the East Siberian Sea is a source region for this basin-wide change in sea-ice thickness distribution (e.g. see fig. 11 of Rothrock et al., 2003). This region also experiences the largest amount of interannual variation in the summer SIC field (see fig. 14 of Deser et al., 2000), which may be indicative of strong atmospheric forcing. These model results and observations suggest that atmospheric circulation over the East Siberian Sea and its vicinity plays a crucial role both in the dynamical mechanism proposed by Rigor and Wallace (2004) and in the formation of the Arctic frontal zone (Serreze et al., 2001). A question then arises, in the context of a potential dynamical link between winter and summer sea-ice conditions, as to how the aforementioned lag relationship of the regional SIEs over Eurasia (from the Nordic to Okhotsk Seas) is related to summertime atmospheric conditions over the coastal region of Siberia, in particular over the East Siberian Sea. A key issue is whether or not anomalous atmospheric circulation in summer, which is associated with a below-normal Nordic SIE in the previous winter and a below-normal Okhotsk SIE in the subsequent winter, provides favourable conditions for a summertime sea-ice reduction in the East Siberian Sea and its vicinity.

To examine this issue, we constructed two sets of composites of SLP anomalies for each of the months from May to September. One composite is for summers with below-normal Nordic SIE in the previous winter and with below-normal Okhotsk SIE in the subsequent winter. The other composite consists of summers with above-normal Nordic SIE in the previous winter and with above-normal Okhotsk SIE in the subsequent winter. A comparison reveals that the June SLP composite for the below-normal

Nordic SIE in the previous winter and the below-normal Okhotsk SIE in the subsequent winter exhibits positive SLP anomalies over eastern Siberia and the Sea of Okhotsk (Fig. 6a), while the SLP anomalies are weakly negative in the counterpart with the above-normal Nordic and Okhotsk SIEs (Fig. 6b). This feature with positive anomalies over the eastern Siberia–Okhotsk region is recognized as a manifestation of the frequent occurrence of the surface Okhotsk high, which has been discussed previously in the context of the formation and enhancement of the Arctic frontal zone (Nakamura and Fukamachi, 2004; Ogi et al., 2004a, 2004b; Tachibana et al., 2004).

The above results indicate that the Okhotsk high tends to occur during a summer preceded by a below-normal Nordic SIE and followed by a below-normal Okhotsk SIE, which in turn could affect the central Arctic sea-ice cover. A persistently low Nordic SIE may occur as a response to a positive-NAO forcing through climatic memory and persistence over the subpolar North Atlantic. It is then conceivable that an NAO-related atmospheric forcing in the North Atlantic may have prolonged influences on summer sea-ice conditions in the East Siberian Sea and the central Arctic Ocean. Changes in radiative and/or oceanic conditions in addition to an ice-albedo feedback may well be significant factors for the downward trends in the summer SIE over the Arctic Ocean. Nonetheless, on the basis of our results we hypothesize that a climate memory, particularly over the North Atlantic region and over Eurasia, transforms atmospheric forcing effects at interannual and shorter time-scales into changes in sea-ice conditions at longer time-scales.

4.3. Tropical influence

The Pacific signatures of Figs. 2 (second and third rows) and 3 suggest that the observed west-to-east evolving pattern of anomalies may originate in the Pacific sector or at least be linked to atmospheric variability in the North Pacific. For example, the SLP anomalies in Fig. 2g resemble the surface manifestation of the Pacific-North American (PNA) teleconnection pattern defined by Wallace and Gutzler (1981). Since the remote influence of El Niño-Southern Oscillation (ENSO) has some projection on the PNA pattern (e.g. Horel and Wallace, 1981; Trenberth, 1990), it is natural to address a link between ENSO and the observed eastward pattern of sea-ice signals especially in light of an emerging view that ENSO modulates climate variability in the southern high latitudes (e.g. Marshall and King, 1998; Yuan and Martinson, 2000; Turner, 2004, and references therein).

For the NH, atmospheric general circulation model experiments suggest that positive SST anomalies in the tropics, especially in the Indo-Pacific region, tend to force the NAO towards its positive polarity (e.g. Hoerling et al., 2004; Hurrell et al., 2004 and references therein). The response of the North Atlantic storm track to remote tropical forcing has been proposed as a possible mechanism (Lu et al., 2004 and references therein).

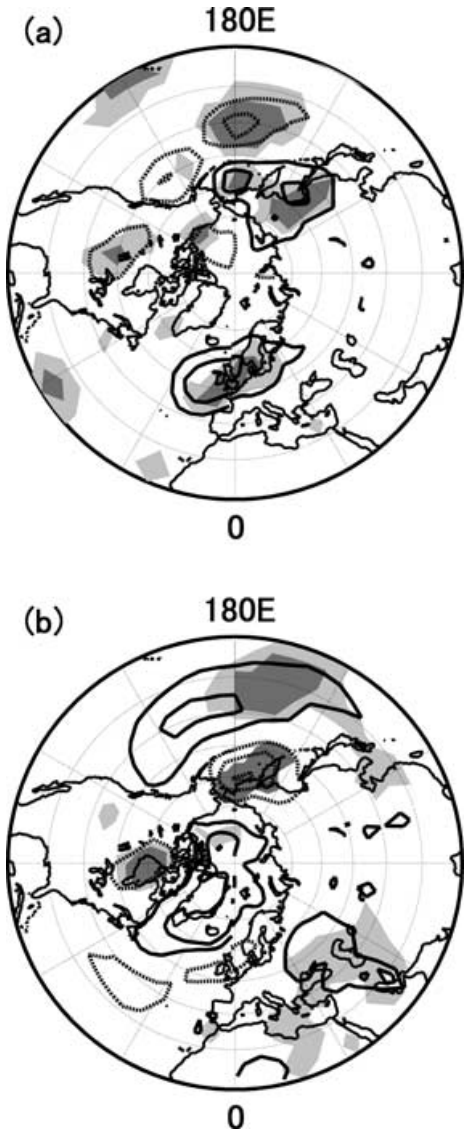

Fig. 6. Composites of June SLP anomalies. (a) Composite of summers (June) with below-normal Nordic SIE in the previous winter and below-normal Okhotsk SIE in the subsequent winter. (b) Composite of summers with above-normal Nordic SIE in the previous winter and above-normal Okhotsk SIE in the subsequent winter. The years included in the composites are 1973, 1975, 1983, 1990 and 1995 for (a) and 1978, 1979, 1981, 1982, 1987 and 1999 for (b). These years were selected using the criteria of below -0.5 and above $+0.5$ standard deviations on the normalized Vinje's Barents and JMA's Okhotsk SIE time-series. The shading indicates areas of $>95\%$ (dark) and $>90\%$ (light) confidence levels based on a Monte Carlo procedure with 500 random composites.

Observations are in general supportive of the presence of such a tropical link to the positive polarity of the NAO during the cold phase of ENSO, which is referred to as La Niña (e.g. Fraedrich, 1990; Dong et al., 2000; Cassou and Terray, 2001; Pozo-Vazquez et al., 2001 among others). In association with La Niña, PNA

tends to be in its negative phase with an anomalously weak Aleutian low (e.g. Trenberth et al., 1990). Thus, the teleconnection pattern of La Niña may be characterized by a weakened Aleutian low and an intensified Icelandic low, although this characterization does not have a reversed pattern during El Niño events due to non-linearity in remote tropical forcing (Lu et al., 2004). This pattern of the weaker Aleutian low with the stronger Icelandic low is evident not only in the SLP composite for La Niña events (e.g. see fig. 2 of Pozo-Vazquez et al., 2001), but also in our maps of DJF-averaged SLP anomalies regressed both on the PC1-SIE and on regional SIE time-series with the maximum lag of two winters (third row of Fig. 2). It cannot entirely be ruled out that these similarities are statistical artefacts. However, an empirical relationship between La Niña and the positive polarity of the NAO appears significant over an extended period of time (e.g. Pozo-Vazquez et al., 2001 analysed data for the entire twentieth century). Evidence is also emerging from both model simulations and observations for delayed and prolonged influences of the positive phase of the NAO on sea-ice. On the basis of our results, it is not unreasonable to conjecture a tropical link to variations and changes in NH sea-ice conditions including recent downward trends. Future work is clearly needed to scrutinize this conjecture with the goal of attaining a better mechanistic understanding of the lags and of the propagation of climatic anomalies in the northern high latitudes from a global perspective. Towards this goal, we suggest numerical studies using a fully coupled atmosphere–ice–ocean model to examine climate interactions between low latitudes and high latitudes with an emphasis on the propagation of climate anomalies in high latitudes especially over the North Atlantic and Eurasia.

5. Summary

Through analyses of fully hemispheric sea-ice data, this study has revealed a highly coherent spatial and temporal structure of NH wintertime sea-ice variability and its close link to anomalous atmospheric circulation and sea-ice trends in recent decades. First, the dominant mode of wintertime sea-ice variability defined through an EOF analysis represents sea-ice variations concentrated in the sub-Arctic regions. It appears robust with respect to sea-ice records of varying time periods and from different sources (e.g. Chapman and Walsh, 1996; Cavalieri et al., 1997; Deser et al., 2000; Partington et al., 2003). The mode is characterized by a double-dipole pattern composed of one dipole over the North Atlantic and the other over the North Pacific. These sea-ice dipoles over the two ocean basins are significantly correlated with one another on interannual time-scales. Secondly, there is a significant lag relationship between anomalous SIE and North Atlantic atmospheric variations. The lagged correlation between the NAO and the leading mode of sea-ice variability is significant when the former leads at lags up to two winters. Anomalous atmospheric circulation associated with this two-year lag relationship has a pattern that is reminiscent of the AO with a clear North Pacific signature. Thirdly, there are significant lag relationships between regional SIEs, which are indicative of an eastward evolving pattern of the sea-ice signals at regional scales: one from the Labrador Sea to the Nordic Seas over one winter, and the other from the Nordic Seas to the Sea of Okhotsk over another winter. Fourthly, our findings on the lag structure of sea-ice anomalies and associated anomalies in atmospheric circulation appear to be critical for the downward sea-ice trends in both summer and winter. Finally, our results suggest a tropical link to changes in the NH sea-ice conditions in recent decades.

6. Acknowledgments

We thank H. Goosse, G. Kukla, Y. Kushnir, D. Martinson, T. Vinje, M. Watanabe, X. Yuan, and anonymous reviewers for many helpful comments and T. Mikami for assistance. This research was supported in part by NASA's cryosphere program and the Japanese Ministry of Education, Culture, Sports, Science and Technology. This is Lamont-Doherty Earth Observatory contribution 7002.

References

Aagaard, K. and Carmack, E. C. 1989. The role of sea ice and other fresh waters in the Arctic circulation. *J. Geophys. Res*. **94**, 14485–14498.

Bengtsson, L., Semenov, V. A. and Johannessen, O. M. 2004. The early twentieth-century warming in the Arctic – A possible mechanism. *J. Climate* **17**, 4045–4057.

Blindheim, J., Borovkov, V., Hansen, B., Malmberg, S.-Aa., Turrell, W. R. and co-authors. 2000. Upper layer cooling and freshening in the Norwegian Sea in relation to atmospheric forcing. *Deep-Sea Res.* **47**, 655–680.

Bojariu, R. and Gimeno, L. 2003. The role of snow cover fluctuations in multiannual NAO persistence. *Geophys. Res. Lett*. **30**, 1156, doi:10.1029/2002GL01651.

Cassou, C. and Terry, L. 2001. Dual influence of Atlantic and Pacific SST anomalies on the North Atlantic/Europe winter climate. *Geophys. Res. Lett*. **28**, 3195–3198.

Cavalieri, D. J., Gloersen, P., Parkinson, C. L., Comiso, J. C. and Zwally, H. J. 1997. Observed hemispheric asymmetry in global sea ice changes. *Science* **278**, 1104–1106.

Cavalieri, D. J., Parkinson, C. L., Gloersen, P., Comiso, J. C. and Zwally, H. J. 1999. Deriving long-term time series of sea ice Cover from satellite passive-microwave multisensor data sets. *J. Geophys. Res.* **104**, 15803–15814.

Cavalieri, D. J., Parkinson, C. L. and Vinnikov, K. Y. 2003. 30-year satellite record reveals contrasting Arctic and Antarctic decadal sea ice variability. *Geophys. Res. Lett*. **30**, 1970, doi:10:1029/2003GL018031.

Chapman, W. L. and Walsh, J. E. 1993. Recent variations of sea ice and air temperature in high latitudes. *Bull. Am. Meteorol. Soc.* **74**, 33–47.

Cohen, J. and Entekhabi, D. 1999. Eurasian snow cover variability and Northern Hemisphere climate predictability. *Geophys. Res. Lett.* **26**, 345–348.

Comiso, J. C. 2002. A rapidly declining perennial sea ice cover in the Arctic. *Geophys. Res. Lett*. **29**, 1956, doi:10:1029/2002GL015650.

Deser, C., Walsh, J. E. and Timlim, M. S. 2000. Arctic sea ice variability in the context of recent atmospheric circulation trends. *J. Climate* **13**, 617–633.

Deser, C., Holland, M., Reverdin, G. and Timlin, M. 2002. Decadal variations in Labrador Sea ice cover and North Atlantic sea surface temperature. *J. Geophys. Res.* **107**, 10.1029/2000JC000683.

Deser, C., Alexander, M. A. and Timlin, M. S. 2003. Understanding the persistence of sea surface temperature anomalies in midlatitudes. *J. Climate* **16**, 57–72.

Dickson, R. R., Osborn, T. J., Hurrell, J. E., Meincke, J., Blindheim, J. and co-authors. 2000. The Arctic Ocean response to the North Atlantic Oscillation. *J. Climate* **13**, 2671–2696.

Dong, B.-W., Sutton, R. T., Jewson, S. P., O'Neill, A. and Slingo, J. M. 2000. Predictable winter climate in the North Atlantic sector during the 1997-1999 ENSO cycle. *Geophys. Res. Lett.* **27**, 985–988.

Fraedrich, K. 1990. Grosswetter during the warm and cold extremes of the El Nino/Southern Oscillation. *Int. J. Climatol.* **10**, 21–31, 1990.

Hoerling, M. P., Hurrell, J. W., Xu, T., Bates, G. T. and Phillips, A. S. 2004. Twentieth century North Atlantic climate change. Part II: understanding the effect of Indian Ocean warming. *Clim. Dyn.* **23**, 391–405.

Horel, J. D. and Wallace, J. M. 1981. Planetary-scale atmospheric phenomena associated with the Southern Oscillation. *Mon. Wea. Rev.* **109**, 813–829.

Hurrell, J. W. 1995. Decadal trends in the North Atlantic Oscillation: Regional temperatures and precipitation. *Science* **269**, 90–92.

Hurrell, J. W., Hoerling, M. P., Phillips, A. S. and Xu, T. 2004. Twentieth century North Atlantic climate change. Part I: assessing determinism. *Clim. Dyn.* **23**, 371–389.

Ikeda, M. 1990. Decadal oscillations of the air-ice-ocean system in the Northern Hemisphere. *Atmos.-Ocean* **28**, 106–139.

Kauker, F., Rudiger, R., Karcher, M., Koberle, C. and Lieser, J. L. 2003. Variability of Arctic and North Atlantic sea ice: A combined analysis of model results and observations from 1978 to 2001. *J. Geophys. Res.* **108**, 10.1029/2002JC001573.

Lu, J., Greatbatch, R. J. and Peterson, K. A. 2004. Trend in Northern Hemisphere winter atmospheric circulation during the last half of the twentieth century. *J. Climate* **17**, 3745–3760.

Marshall, G. J. and King, J. C. 1998. Southern Hemisphere circulation anomalies associated with extreme Antarctic Peninsula winter temperatures. *Geophys. Res. Lett.* **25**, 2437–2440.

Mysak, L. A. and Venegas, S. A. 1998. Decadal climate oscillations in the Arctic: A new feedback loop for atmosphere-ice-ocean interactions. *Geophys. Res. Lett.* **25**, 3607–3610.

Nakamura, H. and Fukamachi, T. 2004. Evolution and dynamics of summertime blocking over the Far East and the associated surface Okhotsk high. *Quart. J. Roy. Meteor. Soc.* **130**, 1213–1233.

Niebauer, H. J. 1998. Variability in Bering Sea ice cover as affected by a regime shift in the North Pacific in the period of 1947-1996. *J. Geophys. Res.* **103**, 27717–27737.

Ogi, M., Tachibana, Y. and Yamazaki, K. 2004a. The connectivity of the winter North Atlantic Oscillation (NAO) and the summer Okhotsk high. *J. Meteo. Soc. Japan* **82**, 905–913.

Ogi, M., Ymazaki, K. and Tachibana, Y. 2004b. The summertime annular mode in the Northern Hemisphere and its linkage to the winter mode. *J. Geophys. Res.* **109**, 10.1029/2004JD004514.

Overland, J. E. and Turet, P. 1994. Variability of the atmospheric energy flux across 70°N computed from the GFDL data set. *Geophys. Monogr.* **84**, AGU, 313–325.

Parkinson, C. L. 1990. The impact of the Siberian high and Aleutian low on the sea-ice cover of the Sea of Okhotsk. *Ann. Glaciol.* **14**, 226–229.

Parkinson, C. L. 2000. Recent trend reversals in Arctic sea ice extents: Possible connections to the North Atlantic Oscillation. *Polar Geography* **24**, 1–12.

Parkinson, C. L., Cavalieri, D. J., Gloersen, P., Zwally, H. J. and Comiso, J. C. 1999. Arctic sea ice extents, areas, and trends, 1978-1996. *J. Geophys. Res.* **104**, 20837–20856.

Partington, K., Flynn, T., Lamb, D., Bertoia, C. and Dedrick, K. 2003. Late twentieth century Northern Hemisphere sea-ice record from U. S. National Ice Center ice charts. *J. Geophys. Res.* **108**, doi:10.1029/2002JC001623.

Pozo-Vazquez, D., Esteban-Parra, M. J., Radrigo, F. S. and Castro-Diez, Y. 2001. The association between ENSO and winter atmospheric circulation and temperature in the North Atlantic region. *J. Climate* **14**, 3408–3420.

Rigor, I. G. and Wallace, J. M. 2004. Variations in the age of Arctic sea-ice and summer sea-ice extent. *Geophys. Res. Lett.* **31**, doi:10.1029/2004GL019492.

Robock, A., Mu, M., Vinnikov, K. and Robinson, R. 2003. Land surface conditions over Eurasia and Indian summer monsoon rainfall. *J. Geophys. Res.* **108**, doi: 10.1029/2002JD002286.

Rogers, J. C. and van Loon, H. 1979. The seesaw in winter temperatures between Greenland and northern Europe. Part II Some oceanic and atmospheric effects in middle and high latitudes. *Mon. Wea. Rev.* **107**, 509–519.

Rothrock, D. A., Zhang, J. and Yu, Y. 2003. The Arctic ice thickness anomaly of the 1990s: A consistent view from observations and models. *J. Geophys. Res.* **108**, doi:10.1029/2001JC001208.

Serreze, M. C., Walsh, J. E., Chapin, F. S. III, Osterkamp, T., Dyurgerov, M. and co-authors 2000. Observational evidence of recent change in the northern high-latitude environment. *Climatic Change* **46**, 159–207.

Serreze, M. C., Lynch, A. H. and Clark, M. P. 2001. The Arctic frontal zone as seen in the NCEP-NCAR reanalysis. *J. Climate* **14**, 1550–1567.

Stroeve, J., Serreze, M. C., Fetterer, F., Arbetter, T., Meier, W. and co-authors. 2005. Tracking the Arctic's shrinking ice cover: Another extreme September minimum in 2004. *Geophys. Res. Lett.*, **32**, doi:10.1029/2004GL021810.

Tachibana, Y., Iwamoto, T. and Ogi, M. 2004. Abnormal meridional temperature gradient and its relation to the Okhotsk high. *J. Met. Soc. Japan*, **82**, 1399–1415.

Thompson, D. J. W. and Wallace, J. M. 1998. The Arctic Oscillation in the wintertime geopotential height and temperature fields. *Geophys. Res. Lett.* **25**, 1297–1300.

Trenberth, K. E. 1990. Recent observed interdecadal climate changes in the Northern Hemisphere. *Bull. Am. Meteorol. Soc.* **71**, 988–992.

Trenberth, K. E. and Paolino, D. A. 1980. The Northern Hemisphere sea level pressure data set: Trends, errors, and discontinuities. *Mon. Wea. Rev.* **108**, 855–872.

Turner, J. 2004. The El Niño-Southern Oscillation and Antarctica. *Int. J. Climatol.* **24**, 1–31.

van Loon, H. and Rogers, J. C. 1978. The seesaw in winter temperatures between Greenland and northern Europe. Part I General description. *Mon Wea. Rev.* **106**, 296–310.

Vinje, T. 2001. Anomalies and trends of sea-ice extent and atmospheric circulation in the Nordic Seas during the period 1864-1998. *J. Climate* **14**, 255–267.

Wallace, J. M. 2000. North Atlantic Oscillation/annular mode: Two paradigms – one phenomenon. *Q. J. R. Meteorol. Soc.* **126**, 791–805.

Wallace, J. M. and Gutzler, D. S. 1981. Teleconnections in the geopotential height field during the Northern Hemisphere winter. *Mon. Wea. Rev.* **109**, 784–812.

Walsh, J. E., Chapman, W. L. and Shy, T. L. 1996. Recent decrease of sea level pressure in the central Arctic. *J. Climate* **9**, 480–486.

Watanabe, M. and Nitta, T. 1998. Relative importance of snow and sea surface temperature anomalies on an extreme phase in the winter atmospheric circulation. *J. Climate* **11**, 2837–2857.

Watanabe, M. and Nitta, T. 1999. Decadal changes in the atmospheric circulation and associated surface climate variations in the Northern Hemisphere. *J. Climate* **12**, 494–510.

Wijffels, S. E., Schmitt, R. W., Bryden, H. L. and Stigebrandt, A. 1992. Transport of freshwater by the oceans. *J. Phys. Oceanogr.* **22**, 155–162.

Yuan, X. and Martinson, D. G. 2000. Antarctic sea ice extent variability and its global connectivity. *J. Climate* **13**, 1697–1717.